

Analytical solution of viscous microfluid flow inside an evaporating sessile drop: Cylindrical and spherical cap shape

Hassan Masoud*

Department of Mechanical and Aerospace Engineering, State University of New York at
Buffalo, Buffalo, New York 14260, USA

The 3D axisymmetric and 2D time-dependent flow field inside an evaporating sessile droplet whose contact line is pinned is studied analytically with a free-shear boundary condition on the surface of the droplet at low capillary and Bond numbers. Solutions are obtained for *arbitrary* contact angle ($0 \leq \theta_c \leq \pi/2$) and non uniform evaporation rate. Fourier sine transform and transform introduced in (H. Masoud, Physical Review E, in review (2008)) based on Gegenbauer function are used respectively for solving 2D and 3D axisymmetric problems. Published solutions of evaporation rate considered only diffusion as the transport mechanism. The analysis was corrected to allow for the actual convective-diffusive behavior. It is also shown that infinite evaporation rate predicted by solving Laplace's equation for the vapor phase is not tolerable and needs to be modified.

I. INTRODUCTION

There is a rapidly growing technological and scientific interest in fluid mechanics and mass transport during droplet evaporation. "Sessile drop evaporation is commonly found in industrial and scientific processes including the evaporation of droplets of ink or paint

* Master student; Electronic address: hmasoud@eng.buffalo.edu

on the surface of paper and the evaporation of suspensions of nanoparticles or biomolecules on a solid substrate [1-3]. Lately, there is increasing interest in using drop evaporation for particle deposition applications which stimulates the theoretical understanding (preferably with analytical approach) of this drying process. By understanding the evaporation dynamics and its effect on the fluid flow, the particle deposition profile on the substrate during drop drying can be predicted, hence may lead to the understanding on how to control the particle deposition during drop drying.”, reported in [4]. As Explained in [5], “Under evaporation, a drop of colloidal suspension or solution having a strongly anchored three-phase line, keeps a cylindrical or spherical cap shape with a constant base. The contact angle decreases with time and the height in each point of the profile decreases. To satisfy the anchoring condition, a flow of liquid has to occur inside the drop. An outward flow in a drying drop is produced when the contact line is pinned so that liquid removed by evaporation from the edge of the drop must be replenished by a flow of liquid from the interior. This flow is capable of transferring most of the solute to the contact line and thus accounts for the strong perimeter concentration of many stains.”

Summarized literature survey in [6] says, “Several attempts to describe the internal flow during droplet evaporation have been reported in the literature and can be, in general, divided in two main categories. In the first one, the flow field in the interior of the droplet is determined through analytical, approximate analytical and numerical solutions, whereas in the second, only the vertically averaged liquid velocity is calculated, which nevertheless provides a useful picture of the mean microflow. In the former case, analytical solutions were provided assuming a cylindrical [7] and spherical

[8] cap geometry and potential flow conditions inside the droplet.” In addition recently numerical [9] and approximate analytical [10] solutions in the limit of lubrication theory (thin droplets) and numerical study of the Stokes flow (with arbitrary contact angle) [10,11] for the flow field have been investigated. In the second case, the vertically averaged velocity is calculated from a mass balance [12,13] without any detailed information on the local flow field.

In the present work assumption of potential flow is removed and analytical solution of the Stokes flow inside an evaporating sessile drop (2D and 3D axisymmetric) is presented. In addition, evaporation rate equation in 3D case is reformulated, in order to consider the effect of Stefan flow [14], and modified in order to remove the singularity at the contact line.

II. MODEL DEVELOPMENT AND SOLUTIONS

As it has been used by [7,8] and can be seen from Fig. 1, the appropriate coordinate systems which fit the boundaries are bipolar (for 2D) and toroidal (for 3D axisymmetric) coordinates. Like Refs. [7-13], it is assumed that the shape of the drop is a spherical (cylindrical) cap. Properly described in [10], “In general, the shape of a sessile drop on a substrate is controlled by a normal-stress balance on the free surface, which is influenced by gravity, fluid flow within the droplet, surface tension, and “vapor recoil” [15] due to acceleration of liquid upon evaporation. When fluid flow is very slow, the capillary number $Ca = \mu V / \sigma$ is small and the surface tension dominates the normal stress balance, so that the shape is that of a static droplet. For small droplets, gravity is also negligible, and this shape is then simply a spherical cap, achieved at small values of

$Bo = \rho g r^2 / \sigma$, which accounts for the balance of surface tension and gravitational force.

Here ρ is the fluid density, g is the gravitational constant, r is the radius of curvature of the free surface, σ is the surface tension of the liquid, μ is the liquid viscosity, and V is some characteristic value of flow velocity. For small water droplets with contact surface radii (half-width) of 0.1-1.0 mm and slow flows (around $1 \mu\text{m/s}$), the Bond number is in the range 0.01-0.04 and the capillary number is around 10^{-8} , so that the spherical (cylindrical) cap approximation is a good one.”

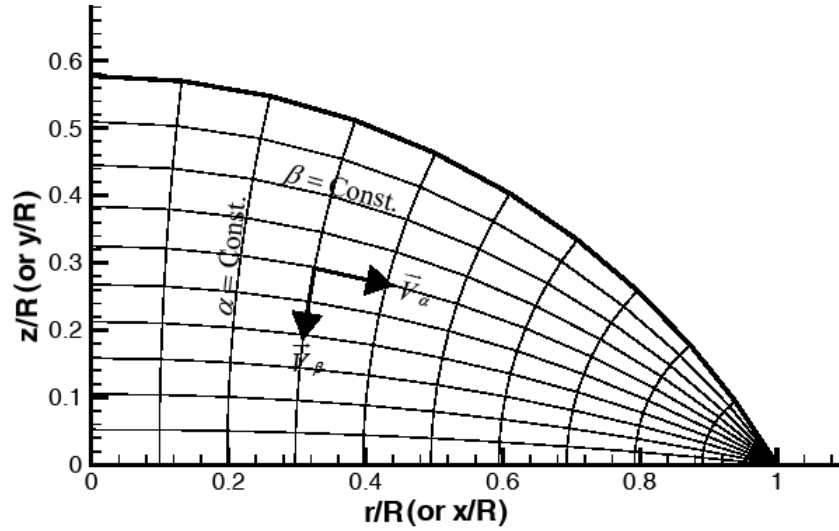


FIG. 1. Lines of constant α and β in toroidal (bipolar) coordinate and positive direction of velocity vector components in toroidal (bipolar) and cylindrical (Cartesian) coordinates.

At the interface between the liquid and the vapor, the vapor concentration is assumed to be equal to the saturation value. Far above the droplet, the vapor concentration approaches an ambient value. The difference in water vapor concentration between the droplet surface and the far-field (diffusion) and also Stefan flow (convection) drives the evaporation of water into the air, according to the vapor conservation equation. Previous studies [12,16,17] neglected convective component but including convective contribution allows higher evaporation rates to be treated. Corrected form of vapor conservation

equation and its solution is provided in appendix A. Reported by [16] because of the low evaporation rate, the dimensionless group R^2 / Dt_f is small (about 10^{-5}), where t_f is the time for the droplet to evaporate and D is the vapor diffusivity. Hence, the vapor concentration field above the droplet can be considered to be at a quasi-steady state. Therefore field equations can be solved without transient term like what has been done in [7-13]. Although equations are solved at a quasi-steady state but it does not mean that the solutions are not time dependent. In all solutions contact angle is involved as a parameter which itself is a function time. Therefore contact angle represents indirectly, time dependency in the solutions.

Continuity and Navier-Stokes equations in low Reynolds number (Stokes or creeping flow) and in the absence of gravity, respectively become

$$\nabla \cdot V = 0 \quad (1)$$

and

$$\mu \nabla^2 V = \nabla P. \quad (2)$$

It is known that in 2D and 3D axisymmetric flows velocity can be expressed in terms of stream function. Stream function is defined in the way that automatically satisfies the continuity equation. Therefore, by using stream function only one partial differential equation needs to be solved rather than two, and this makes the problem a lot easier and analytically solvable. In 2D flow $\nabla^4 \psi = 0$ (biharmonic equation) and in 3D axisymmetric flow $E^4 \psi = 0$ equation has to be solved, where E^2 is the Stokes operator. Further information about low Reynolds number flows can be found in [18]. $\nabla^4 \psi = 0$ and $E^4 \psi = 0$ equations are solved respectively in part A and B of this section.

A. CYLINDRICAL CAP SHAPE

As mentioned before for 2D case the appropriate coordinate system which fits the boundaries is bipolar coordinates. In the bipolar coordinates, the location of a point is given by the coordinates α, β (or $\theta = \pi - \beta$), z where, the Cartesian coordinates are

$$(x, y, z) = (R \frac{\sinh \alpha}{\cosh \alpha + \cos \theta}, R \frac{\sin \theta}{\cosh \alpha + \cos \theta}, z), \quad (3)$$

and R is the half-width of contact surface. As a result, Laplace's equation in this coordinate system becomes

$$\frac{(\cosh \alpha + \cos \theta)^2}{R^2} \left(\frac{\partial^2 \psi}{\partial \alpha^2} + \frac{\partial^2 \psi}{\partial \theta^2} \right) = 0, \quad (4)$$

and based on the definition of stream function which satisfies continuity equation,

$$V_\alpha(\alpha, \theta) = \frac{\cosh \alpha + \cos \theta}{R} \frac{\partial \psi}{\partial \theta} \quad (5)$$

and

$$V_\beta(\alpha, \theta) = \frac{\cosh \alpha + \cos \theta}{R} \frac{\partial \psi}{\partial \alpha}. \quad (6)$$

For more information about this coordinate system see [18-20]. Suggested by [21], taking

$\phi = (\cosh \alpha + \cos \theta) \psi$ as the dependant variable we have

$$R^2 \nabla^2 \psi = (\cosh \alpha + \cos \theta) \left(\frac{\partial^2 \phi}{\partial \alpha^2} + \frac{\partial^2 \phi}{\partial \theta^2} \right) - 2 \sinh \alpha \frac{\partial \phi}{\partial \alpha} + 2 \sin \theta \frac{\partial \phi}{\partial \theta} + (\cosh \alpha - \cos \theta) \phi. \quad (7)$$

Repeating the operator, a little algebra shows that $\nabla^4 \psi = 0$ leads to

$$\frac{\partial^4 \phi}{\partial \alpha^4} + 2 \frac{\partial^4 \phi}{\partial \alpha^2 \partial \theta^2} + \frac{\partial^4 \phi}{\partial \theta^4} - 2 \frac{\partial^2 \phi}{\partial \alpha^2} + 2 \frac{\partial^2 \phi}{\partial \theta^2} + \phi = 0. \quad (8)$$

From the solution of Laplace's equation for potential flow [7], it is obvious that $\sin(\tau\alpha)$ is the eigenfunction, which is of course in α direction, and $\tau \geq 0$ is its corresponding eigenvalue. This means that the solution has to be of the type $\phi = T(\theta)\sin(\tau\alpha)$, (6) shows that the differential equation for $T(\theta)$ is

$$\frac{d^4 T}{d\theta^4} + 2(1 - \tau^2) \frac{d^2 T}{d\theta^2} + (\tau^2 + 1)^2 T = 0,$$

the solution of which is

$$T(\theta) = C(\tau)\cos[(i\tau + 1)\theta] + D(\tau)\cos[(i\tau - 1)\theta] + E(\tau)\sin[(i\tau + 1)\theta] + F(\tau)\sin[(i\tau - 1)\theta]. \quad (9)$$

Therefore, the general solution can be written as

$$\psi(\alpha, \theta; \theta_c) = \frac{1}{\cosh \alpha + \cos \theta} \int_0^\infty k(\tau, \theta; \theta_c) \sin(\tau\alpha) d\tau, \quad (10)$$

where,

$$k(\tau, \theta; \theta_c) = C(\tau; \theta_c) \cos[(i\tau + 1)\theta] + D(\tau; \theta_c) \cos[(i\tau - 1)\theta] + E(\tau; \theta_c) \sin[(i\tau + 1)\theta] + F(\tau; \theta_c) \sin[(i\tau - 1)\theta].$$

The unknown coefficients (C , D , E and F) can be potentially complex functions and are determined subject to the following boundary conditions:

no penetration and zero derivative of V_β in α direction on the axis of symmetry

$$V_\alpha(0, \theta) = 0 \quad \text{or} \quad \psi(0, \theta) = 0, \quad (11)$$

$$\frac{\partial V_\beta}{\partial \alpha} = 0, \quad (12)$$

no slip condition on the solid surface

$$V_\beta(\alpha, 0) = 0 \quad \text{or} \quad \psi(\alpha, 0) = 0, \quad (13)$$

$$V_{\alpha}(0, \theta) = 0 \quad \text{or} \quad \frac{\partial \psi}{\partial \theta}(0, \theta) = 0, \quad (14)$$

finite value at the contact line

$$\psi(\infty, \theta) = \text{finite}, \quad (15)$$

$$\frac{\partial \psi}{\partial \alpha} \psi(\infty, \theta) = \text{finite}, \quad (16)$$

local mass conservation and zero shear stress at the surface

$$V_{\beta}(\alpha, \theta_c; \theta_c) = V_{\text{normal-interface}}(\alpha; \theta_c) - \frac{J(\alpha; \theta_c)}{\rho_{\text{drop}}}, \quad (17)$$

$$\tau_{\alpha\beta}(\alpha, \theta_c; \theta_c) = 0, \quad (18)$$

Eq. (17) is given in terms of evaporation rate $J(\alpha; \theta_c)$ and the normal component of the surface velocity $V_{\text{normal-interface}}(\alpha; \theta_c)$, where ρ_{drop} is the fluid density and θ_c is the contact angle which itself is a function of time. Using the definition of V_{β} , distribution of stream function on the surface is

$$\psi(\alpha, \theta_c; \theta_c) = f(\alpha; \theta_c) = \int_0^{\alpha} \frac{R}{\cosh \alpha' + \cos \theta_c} V_{\beta}(\alpha', \theta_c; \theta_c) d\alpha'. \quad (19)$$

Knowing that $\frac{R}{\cosh \alpha + \cos \theta}$ is the scale factor in β direction

$$V_{\text{normal-interface}}(\alpha; \theta_c) = -\frac{d\theta_c}{dt} \frac{R}{\cosh \alpha + \cos \theta_c}. \quad (20)$$

Although it has been claimed in [17] that Laplace's equation is solved analytically for the vapor concentration, it is known that there is no analytical solution for Laplace's equation outside the cylindrical cap drop with one boundary at infinity (well known logarithm problem). Therefore, unlike 3D axisymmetric case there is no analytical

expression for evaporation rate in 2D case. Given the evaporation rate (e.g., from the experiment), we finally get

$$f(\alpha; \theta_c) = -\frac{d\theta_c}{dt} \int_0^\alpha \frac{R^2}{(\cosh \alpha' + \cos \theta_c)^2} d\alpha' - \frac{1}{\rho_{drop}} \int_0^\alpha \frac{RJ(\alpha'; \theta_c)}{\cosh \alpha' + \cos \theta_c} d\alpha',$$

which reduces to

$$f(\alpha; \theta_c) = -\frac{d\theta_c}{dt} \frac{R^2}{\sin^2 \theta_c} \left\{ \frac{\sinh \alpha}{\cosh \alpha + \cos \theta_c} + \cot \theta_c \left[\sin^{-1} \left(\frac{1 + \cosh \alpha \cos \theta_c}{\cosh \alpha + \cos \theta_c} \right) - \frac{\pi}{2} \right] \right\} - \frac{R}{\rho_{drop}} \int_0^\alpha \frac{J(\alpha'; \theta_c)}{\cosh \alpha' + \cos \theta_c} d\alpha', \quad (21)$$

Considering (11), stream function is zero at the contact line ($f(\infty; \theta_c) = 0$). Therefore,

$$\frac{d\theta_c}{dt}(\theta_c) = -\frac{1}{R \rho_{drop}} \frac{\sin^2 \theta_c}{1 - \theta_c \cot \theta_c} \int_0^\infty \frac{J(\alpha; \theta_c)}{\cosh \alpha + \cos \theta_c} d\alpha. \quad (22)$$

In order to express Eq. (16) in terms of stream function, first, stress tensor has to be transformed into bipolar coordinates. General definition of stress tensor, regardless of the coordinate system is

$$\tau = -P\mathbf{I} + \mu \left[\nabla V + (\nabla V)^T \right], \quad (23)$$

where, \mathbf{I} is the identity tensor and the superscript T denotes the transpose. From this, it is clear that

$$\tau_{\alpha\beta} = \nabla V_{12} + \nabla V_{21}, \quad (24)$$

where subscripts denote the element number in the velocity gradient tensor. Using the general formulation of velocity gradient tensor in curvilinear coordinate systems provided by [18], Eq. (22) becomes

$$\tau_{\alpha\beta} = \mu \left\{ \frac{\partial}{\partial \alpha} \left[\left(\frac{\cosh \alpha + \cos \theta}{R} \right) V_{\beta} \right] - \frac{\partial}{\partial \theta} \left[\left(\frac{\cosh \alpha + \cos \theta}{R} \right) V_{\alpha} \right] \right\}. \quad (25)$$

Combining (16) and (23), one can write

$$\begin{aligned} \frac{\partial}{\partial \alpha} \left\{ (\cosh \alpha + \cos \theta_c) \left[V_{normal-interface}(\alpha; \theta_c) - \frac{J(\alpha; \theta_c)}{\rho_{drop}} \right] \right\} \\ = \frac{\partial}{\partial \theta} [(\cosh \alpha + \cos \theta_c) V_{\alpha}(\alpha, \theta_c; \theta_c)]. \end{aligned} \quad (26)$$

For ease of writing, the left hand side of (24) thereafter will be called $g(\alpha; \theta_c)$.

It is obvious that the general solution (Eq. (8)) automatically satisfies conditions on the axis of symmetry (Eq.'s (9), (10)) and at the contact line (Eq.'s (13), (14)). Applying no slip boundary conditions, it is obtained that

$$C(\tau; \theta_c) + D(\tau; \theta_c) = 0 \quad (27)$$

and

$$(i\tau + 1)E(\tau; \theta_c) + (i\tau - 1)F(\tau; \theta_c) = 0. \quad (28)$$

Using (27) and (28) and little more manipulations, $k(\tau, \theta; \theta_c)$ reduces to

$$k(\tau, \theta; \theta_c) = A(\tau; \theta_c) \sin \theta \sinh(\tau \theta) + B(\tau; \theta_c) [\cos \theta \sinh(\tau \theta) - \tau \sin \theta \cosh(\tau \theta)], \quad (29)$$

where, A and B are real functions. Now two equations and two unknown coefficients are left. These equations are

$$f(\alpha; \theta_c) (\cosh \alpha + \cos \theta) = \int_0^{\infty} k(\tau, \theta_c; \theta_c) \sin(\tau \alpha) d\tau \quad (30)$$

and

$$\frac{R g(\alpha; \theta_c)}{\cosh \alpha + \cos \theta_c} - \cos \theta_c f(\alpha; \theta_c) = h(\alpha; \theta_c) = \int_0^{\infty} \kappa(\tau; \theta_c) \sin(\tau \alpha) d\tau, \quad (31)$$

where, $\kappa(\tau; \theta_c) = \frac{\partial^2}{\partial \theta^2} [k(\tau, \theta_c; \theta_c)]$ is

$$A(\tau; \theta_c) \left[(\tau^2 - 1) \sin \theta_c \sinh(\tau \theta_c) + 2\tau \cos \theta_c \cosh(\tau \theta_c) \right] \\ - B(\tau; \theta_c) (\tau^2 + 1) \left[\cos \theta_c \sinh(\tau \theta_c) + \tau \sin \theta_c \cosh(\tau \theta_c) \right]. \quad (32)$$

Using Fourier sine transform

$$k(\tau, \theta_c; \theta_c) = \frac{2}{\pi} \int_0^\infty f(\alpha; \theta_c) (\cosh \alpha + \cos \theta_c) \sin(\tau \alpha) d\alpha, \quad (33)$$

and

$$\kappa(\tau; \theta_c) = \frac{2}{\pi} \int_0^\infty h(\alpha; \theta_c) \sin(\tau \alpha) d\alpha. \quad (34)$$

Therefore,

$$A(\tau; \theta_c) = \frac{N_2(\tau; \theta_c) k(\tau, \theta_c; \theta_c) + N_1(\tau; \theta_c) \kappa(\tau; \theta_c)}{N_2(\tau; \theta_c) M_1(\tau; \theta_c) + N_1(\tau; \theta_c) M_2(\tau; \theta_c)}, \quad (35)$$

and

$$B(\tau; \theta_c) = \frac{M_2(\tau; \theta_c) k(\tau, \theta_c; \theta_c) - M_1(\tau; \theta_c) \kappa(\tau; \theta_c)}{N_2(\tau; \theta_c) M_1(\tau; \theta_c) + N_1(\tau; \theta_c) M_2(\tau; \theta_c)}, \quad (36)$$

where,

$$M_1(\tau; \theta_c) = \sin \theta_c \sinh(\tau \theta_c), \quad (37)$$

$$M_2(\tau; \theta_c) = (\tau^2 - 1) \sin \theta_c \sinh(\tau \theta_c) + 2\tau \cos \theta_c \cosh(\tau \theta_c), \quad (38)$$

$$N_1(\tau; \theta_c) = \cos \theta_c \sinh(\tau \theta_c) - \tau \sin \theta_c \cosh(\tau \theta_c), \quad (39)$$

and

$$N_2(\tau; \theta_c) = (\tau^2 + 1) \left[\cos \theta_c \sinh(\tau \theta_c) + \tau \sin \theta_c \cosh(\tau \theta_c) \right]. \quad (40)$$

Simplified expressions for hemicylinder case are available in appendix B.

Components of velocity in α and β direction can be calculated at each point from

$$V_{\alpha}(\alpha, \theta; \theta_c) = \frac{1}{R} \left\{ \sin \theta \psi(\alpha, \theta; \theta_c) + \int_0^{\infty} \frac{\partial}{\partial \theta} [k(\tau, \theta; \theta_c)] \sin(\tau \alpha) d\tau \right\} \quad (41)$$

and

$$V_{\beta}(\alpha, \theta; \theta_c) = -\frac{1}{R} \left[\sinh \alpha \psi(\alpha, \theta; \theta_c) - \int_0^{\infty} k(\tau, \theta; \theta_c) \cos(\tau \alpha) \tau d\tau \right]. \quad (42)$$

If the velocity components in x or y direction is needed it can be obtained by the following relations

$$V_x(\alpha, \theta; \theta_c) = \frac{\partial \psi}{\partial y} = \frac{1}{\cosh \alpha + \cos \theta} \left[V_{\alpha} (1 + \cosh \alpha \cos \theta) - V_{\beta} \sinh \alpha \sin \theta \right] \quad (43)$$

and

$$V_y(\alpha, \theta; \theta_c) = -\frac{\partial \psi}{\partial x} = -\frac{1}{\cosh \alpha + \cos \theta} \left[V_{\alpha} \sinh \alpha \sin \theta + V_{\beta} (1 + \cosh \alpha \cos \theta) \right] \quad (44)$$

B. SPHERICAL CAP SHAPE

The relationship between bipolar and toroidal coordinate systems is identical to relationship between cylindrical and spherical coordinates. Although they might look very similar, usually one is used for 2D and another one for 3D problems. Accordingly, toroidal coordinates is chosen for 3D axisymmetric problem. In the toroidal coordinates, the location of a point is given by the coordinates α, β (or $\theta = \pi - \beta$), ϕ where the cylindrical coordinates are

$$(r, \phi, z) = \left(R \frac{\sinh \alpha}{\cosh \alpha + \cos \theta}, \phi, R \frac{\sin \theta}{\cosh \alpha + \cos \theta} \right) \quad (45)$$

and R is the radius of contact surface. As a result, Stokes equation ($E^2 \psi = 0$) in this coordinate system becomes

$$\frac{\sinh \alpha (\cosh \alpha + \cos \theta)}{R^2} \left[\frac{\partial}{\partial \alpha} \left(\frac{\cosh \alpha + \cos \theta}{\sinh \alpha} \frac{\partial \psi}{\partial \alpha} \right) + \frac{\partial}{\partial \theta} \left(\frac{\cosh \alpha + \cos \theta}{\sinh \alpha} \frac{\partial \psi}{\partial \theta} \right) \right] = 0. \quad (46)$$

Based on the definition of stream function, that satisfies continuity equation,

$$V_\alpha(\alpha, \theta) = \frac{(\cosh \alpha + \cos \theta)^2}{R^2 \sinh \alpha} \frac{\partial \psi}{\partial \theta} \quad (47)$$

and

$$V_\beta(\alpha, \theta) = \frac{(\cosh \alpha + \cos \theta)^2}{R^2 \sinh \alpha} \frac{\partial \psi}{\partial \alpha}. \quad (48)$$

For more information about this coordinate system see [18-20]. Suggested by [22], the ordinary theory of linear partial differential equations with constant coefficients is applicable to an extent sufficient to show that a solution of $E^4 \psi = 0$ is

$$\psi = \psi_1 + \frac{\sin \theta}{\cosh \alpha + \cos \theta} \psi_2, \quad (49)$$

where, ψ_1 and ψ_2 are any solutions of $E^2 \psi = 0$. From author's previous work [8], it is known that $E^2 \psi = 0$ is the governing equation of corresponding irrotational flow and its solutions are

$$\psi_1 = \frac{1}{\sqrt{\cosh \alpha + \cos \theta}} \sinh(\tau \theta) \times C_{\frac{1}{2} + i\tau}^{-\frac{1}{2}}(\cosh \alpha) \quad (50)$$

and

$$\psi_2 = \frac{1}{\sqrt{\cosh \alpha + \cos \theta}} \cosh(\tau \theta) \times C_{\frac{1}{2} + i\tau}^{-\frac{1}{2}}(\cosh \alpha), \quad (51)$$

where, $C_{1/2+i\tau}^{-1/2}(x)$ is Gegenbauer function of first kind (serves as an eigenfunction here) and $\tau \geq 0$ is the eigenvalue. Using Eq.'s (49), (50), (51) and some trigonometric identities, we get

$$\psi(\alpha, \theta; \theta_c) = \frac{1}{(\cosh \alpha + \cos \theta)^{1.5}} \int_0^\infty k(\tau, \theta; \theta_c) \times C_{\frac{1}{2} + i\tau}^{-\frac{1}{2}} (\cosh \alpha) d\tau, \quad (52)$$

where, $k(\tau, \theta; \theta_c)$ is as the same one as obtained in part A and the unknown coefficients (C , D , E and F) involved in that can again be potentially complex functions and are determined subject to exactly the same boundary conditions. Given in the previous work [8], distribution of stream function at the boundary is

$$f(\alpha; \theta_c) = -\frac{R^3}{2} \frac{d\theta_c}{dt} \left[\frac{1}{(1 + \cos \theta_c)^2} - \frac{1}{(\cosh \alpha + \cos \theta_c)^2} \right] - \int_0^\alpha \frac{R^2 \sinh \alpha'}{(\cosh \alpha' + \cos \theta_c)^2} \frac{J(\alpha'; \theta_c)}{\rho_{drop}} d\alpha', \quad (53)$$

where, using the corrected version of evaporation rate calculated in appendix A,

$$\frac{d\theta_c}{dt} = \frac{\rho_{mix} D_{AB} (u_s - u_\infty)}{\rho_{drop} R^2} (1 + \cos \theta_c)^2 \left\{ \frac{\sin \theta_c}{1 + \cos \theta_c} + 4 \int_0^\infty \frac{1 + \cosh 2\theta_c \tau}{\sinh 2\pi \tau} \tanh [(\pi - \theta_c) \tau] d\tau \right\}. \quad (54)$$

Using the general definition of stress tensor in curvilinear coordinate systems, it is seen that the expression of shear stress ($\tau_{\alpha\beta}$) at the surface of drop is the same as one given in part A of this section.

Similar to cylindrical cap case, the general solution automatically satisfies conditions on the axis of symmetry and at the contact line and from no slip boundary conditions gives us

$$k(\tau, \theta; \theta_c) = A(\tau; \theta_c) \sin \theta \sinh(\tau \theta) + B(\tau; \theta_c) [\cos \theta \sinh(\tau \theta) - \tau \sin \theta \cosh(\tau \theta)]. \quad (55)$$

In the same way as 2D problem, A and B are real functions and are determined from the following equations,

$$f(\alpha; \theta_c)(\cosh \alpha + \cos \theta)^{1.5} = \int_0^\infty k(\tau, \theta_c; \theta_c) \times C_{\frac{1}{2}+i\tau}^{-\frac{1}{2}} (\cosh \alpha) d\tau \quad (56)$$

and

$$h(\alpha; \theta_c) = \int_0^\infty \kappa(\tau, \theta_c; \theta_c) \times C_{\frac{1}{2}+i\tau}^{-\frac{1}{2}} (\cosh \alpha) d\tau, \quad (57)$$

where,

$$h(\alpha; \theta_c) = \frac{1}{\sqrt{\cosh \alpha + \cos \theta_c}} \left\{ \frac{R^2 g(\alpha; \theta_c) \sinh \alpha}{\cosh \alpha + \cos \theta_c} - 1.5 f(\alpha; \theta_c) [\cos \theta_c (\cosh \alpha + \cos \theta_c) - 0.5 \sin^2 \theta_c] \right\}. \quad (58)$$

with the same definition of $g(\alpha; \theta_c)$ defined before.

Using transform introduced in [8],

$$k(\tau, \theta_c; \theta_c) = \tau(\tau^2 + 0.25) \tanh(\pi\tau) \int_0^\infty \frac{f(\alpha; \theta_c)(\cosh \alpha + \cos \theta)^{1.5}}{\sinh \alpha} \times C_{\frac{1}{2}+i\tau}^{-\frac{1}{2}} (\cosh \alpha) d\alpha \quad (59)$$

and

$$\kappa(\tau, \theta_c; \theta_c) = \tau(\tau^2 + 0.25) \tanh(\pi\tau) \int_0^\infty \frac{h(\alpha; \theta_c)}{\sinh \alpha} \times C_{\frac{1}{2}+i\tau}^{-\frac{1}{2}} (\cosh \alpha) d\alpha. \quad (60)$$

Eventually like cylindrical cap case, $A(\tau; \theta_c)$ and $B(\tau; \theta_c)$ can be obtained respectively from Eq.'s (35) and (36).

Simplified expressions for hemisphere case are available in appendix B. Components of velocity in α and β direction can be calculated at each point from

$$V_\alpha(\alpha, \theta; \theta_c) = \frac{(\cosh \alpha + \cos \theta)^{1.5}}{R^2 \sinh \alpha} [0.5 \sin \theta \frac{\psi(\alpha, \theta; \theta_c)}{\sqrt{\cosh \alpha + \cos \theta}}$$

$$+\int_0^\infty A(\tau;\theta_c)\tau\cosh(\tau\theta)\times C_{\frac{1}{2}+i\tau}^{-\frac{1}{2}}(\cosh\alpha)d\tau], \quad (61)$$

and

$$V_\beta(\alpha,\theta;\theta_c)=-\frac{(\cosh\alpha+\cos\theta)^{1.5}}{R^2}[0.5\frac{\psi(\alpha,\theta;\theta_c)}{\sqrt{\cosh\alpha+\cos\theta}}+\int_0^\infty A(\tau;\theta_c)\sinh(\tau\theta)\times P_{-\frac{1}{2}+i\tau}(\cosh\alpha)d\tau]. \quad (62)$$

where, $P_{-1/2+i\tau}(x)$ is the conical function of first kind. If the velocity components in r or z direction is needed it can be obtained by the following relations,

$$V_r(\alpha,\theta;\theta_c)=\frac{1}{r}\frac{\partial\psi}{\partial z}=\frac{1}{\cosh\alpha+\cos\theta}[V_\alpha(1+\cosh\alpha\cos\theta)-V_\beta\sinh\alpha\sin\theta] \quad (63)$$

and

$$V_z(\alpha,\theta;\theta_c)=-\frac{1}{r}\frac{\partial\psi}{\partial r}=-\frac{1}{\cosh\alpha+\cos\theta}[V_\alpha\sinh\alpha\sin\theta+V_\beta(1+\cosh\alpha\cos\theta)] \quad (64)$$

III. RESULTS AND DISCUSSION

The flow field behavior in terms of stream lines (contours of dimensionless stream function) for hemicylinder and hemisphere are shown and compared with their corresponding irrotational flow in Fig. 1 and 2 respectively. It is clear from both figures that, because of no slip boundary condition applied in the viscous cases, streamlines have been moved up. As it has been mentioned several times in the literature, Laplace's equation for evaporation rate gives us singularity (infinite evaporation rate) at the contact line for the contact angle less than $\pi/2$ which again everyone has acknowledged that this

singularity is not physical. Solving the problem numerically, no one found this singularity troublesome mathematically and even it has been mentioned that it does not make any problem [23]. But here, it is evident that if $\lim_{\alpha \rightarrow \infty} J(\alpha, \theta_c) \rightarrow \infty$ then

$\lim_{\alpha \rightarrow \infty} (\cosh \alpha + \cos \theta_c) f(\alpha; \theta_c) \rightarrow \infty$ and as a result, both transforms fail to calculate

$k(\tau, \theta_c; \theta_c)$ and $\kappa(\tau, \theta_c; \theta_c)$. In reference [9], although it has not been seen mathematically troublesome but from physical understanding, it has been assumed that evaporation rate decays to zero exponentially near contact line. Mathematics tells us that maximum tolerable case is when $\lim_{\alpha \rightarrow \infty} J(\alpha, \theta_c) = \text{Const.}$ (like hemicylinder and hemisphere).

Fortunately, although evaporation rate diverges at the contact line, the contribution of that near the contact line ($10 \leq \alpha$) is much more less than the contribution of the rest ($0 \leq \alpha < 10$) in the whole droplet evaporation. Therefore, the difference between assuming evaporation rate is constant and assuming it decays to zero when $10 \leq \alpha$ is very less. In this work, except hemisphere and hemicylinder ($0 \leq \theta_c < \pi/2$), it is assumed that evaporation rate decays to zero sufficiently close to the contact line and as it can be seen from Fig. 4-7, very good agreement is obtained with the previous numerical solutions provided in [10,11]. It should be mentioned that getting the solution for the flow field does not resolve the problem fundamentally and the behavior of evaporation rate near the contact line when the contact line is pinned is still an open field to work on.

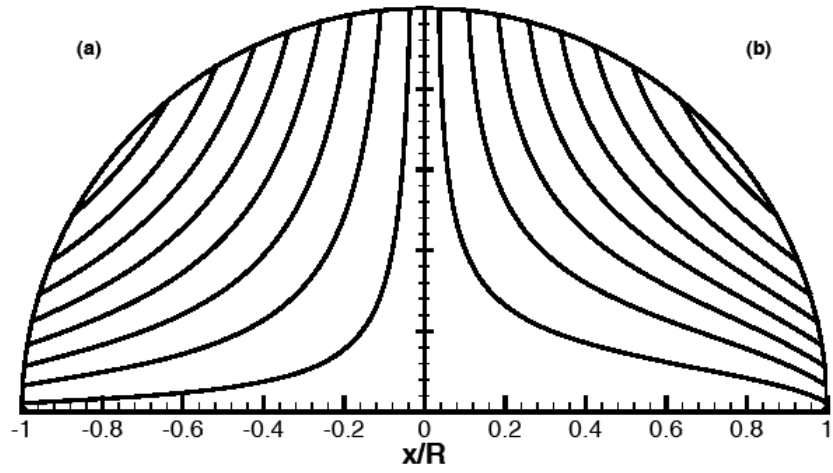


FIG 2. Streamline contours of hemicylinder case (a) potential flow (b) Stokes flow

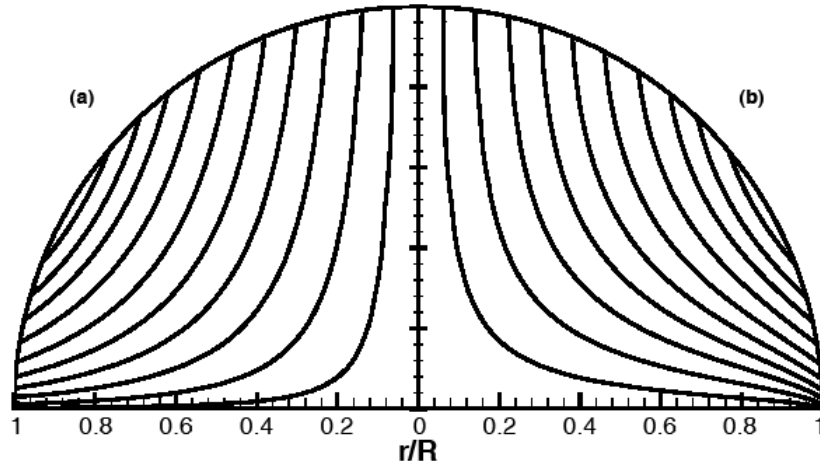


FIG 3. Streamline contours of hemisphere case (a) potential flow (b) Stokes flow

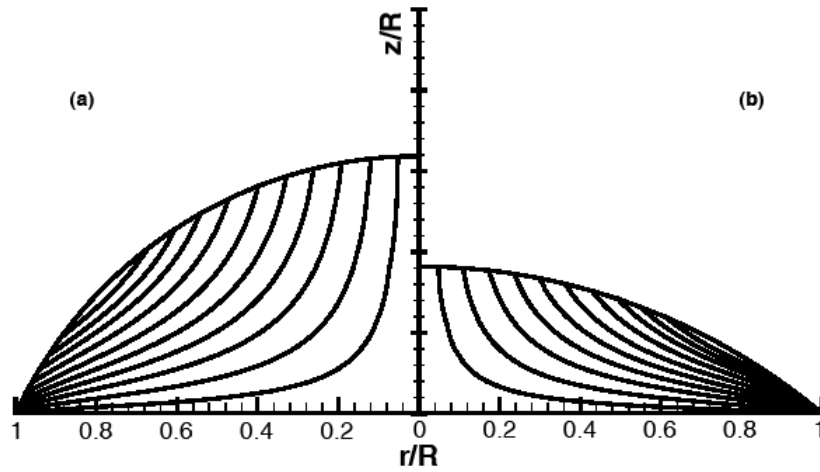


FIG 4. Streamline contours (a) 65° (b) 40°

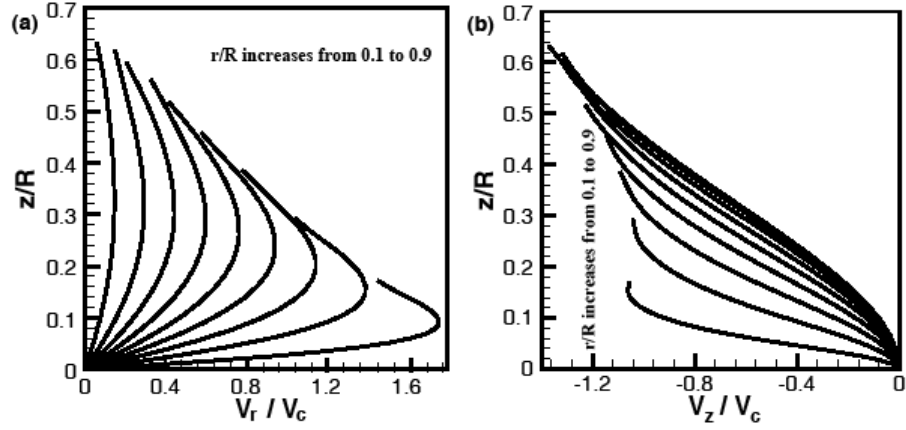


FIG 5. (a) Radial and (b) vertical velocities nondimensionalized by characteristic velocity, $V_c = \frac{\rho_{mix} D_{AB} (u_s - u_\infty)}{\rho_{drop} R}$, versus vertical position at different radial positions $r/R=0.1, 0.3, 0.5, 0.7, 0.9$, for a contact angle of 40° .

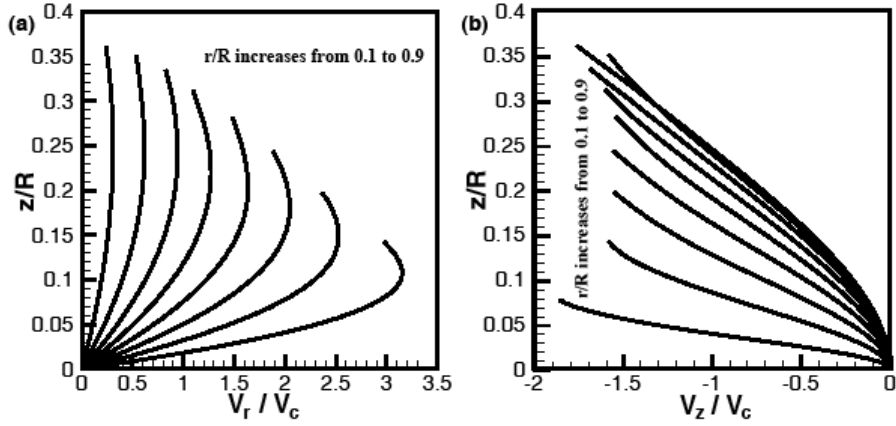


FIG 6. (a) Radial and (b) vertical velocities nondimensionalized by characteristic velocity, $V_c = \frac{\rho_{mix} D_{AB} (u_s - u_\infty)}{\rho_{drop} R}$, versus vertical position at different radial positions $r/R=0.1, 0.3, 0.5, 0.7, 0.9$, for a contact angle of 65° .

Analytical solution of Stokes flow for both 2D and 3D axisymmetric sessile drop with nonuniform evaporation rate and pinned contact line were obtained. Evaporation rate expression also corrected in order to consider the effect of convection. Singularity at the edge of the droplet was investigated from mathematical point of view and practical suggestion is offered in order to skip the singularity. In the future work it is intended to use these two solutions with some improvements and find the analytical solution of Stokes flow inside evaporating sessile drop with *receding* contact line.

ACKNOWLEDGMENT

The study was initiated by Robert C. Wetherhold, who brought the problem to my attention. I gratefully acknowledge helpful discussion with James D. Felske and Ching-Shi Liu and their valuable advices.

APPENDIX A: Evaporation Rate

Basically evaporation rate ($J(\alpha; \theta_c)$) is due to vapor convective-diffusive motion. Even in the cases that evaporation takes place through the stagnant air, convective motion (Stefan flow) is still there. Previous studies [8-13,16,17] neglected convective component which is a reasonable approximation for low evaporation rate liquids but including convective contribution allows higher evaporation rate to be treated. As it can be found in every mass transfer book

$$\rho_{mix} \frac{\partial Y_A}{\partial t} = \nabla \cdot \mathbf{m}_A^g, \quad (A1)$$

$$\mathbf{m}_A^g = -\frac{\rho_{mix} D_{AB} \nabla Y_A}{1 - Y_A}, \quad (A2)$$

where, ρ_{mix} is density of air-vapor mixture, Y_A is vapor mass fraction, D_{AB} is air-vapor diffusion coefficient and \mathbf{m}_A^g is vapor mass flux. In steady or quasi steady state (A1) reduces to

$$\nabla \cdot \mathbf{m}_A^g = 0.$$

By introducing new dependent variable $u = \ln(1 - Y_A)$, we get

$$\nabla^2 u = 0. \quad (A3)$$

Thereafter it is exactly the same Laplace's equation ($\nabla^2 c = 0$) that has been already solved by Lebedev [19]. Just c_s has to be replaced by $u_s = \ln(1 - Y_{A,s})$ and c_∞ has to be replaced by $u_\infty = \ln(1 - Y_{A,\infty})$, where $Y_{A,s}$ and $Y_{A,\infty}$ are vapor mass fraction at the droplet surface (saturation value) and in ambient, respectively. Finally evaporation rate considering Stefan flow becomes

$$J(\alpha; \theta_c) = \frac{\rho_{mix} D_{AB} (u_\infty - u_s)}{R} \left\{ \frac{1}{2} \sin \theta_c + \sqrt{2} (\cosh \alpha + \cos \theta_c)^{3/2} \right. \\ \left. \times \int_0^\infty \frac{\cosh \theta_c \tau}{\cosh \pi \tau} \tanh[(\pi - \theta_c) \tau] \times P_{-\frac{1}{2} + i\tau}(\cosh \alpha) \tau d\tau \right\}. \quad (A4)$$

It is also obvious that if $Y_A \ll 1$, then $u_s \approx -Y_A$ and $\rho_{mix} (u_\infty - u_s) = c_s - c_\infty$ (c is the vapor concentration).

APPENDIX B: Special cases

The purpose of this section is to obtain evaporation rate ($J(\alpha; \theta_c)$), rate of change of contact angle ($\frac{d\theta_c}{dt}$), distribution of stream function at the surface ($f(\alpha; \theta_c)$), $h(\alpha; \theta_c)$ and if possible $k(\tau; \theta_c)$ and $\kappa(\tau; \theta_c)$ for hemicylinder and hemisphere cases. Let us start with hemicylinder. As it has been mentioned in [7], in hemicylinder case like hemisphere one, evaporation rate is constant but unlike hemisphere case the magnitude of evaporation rate is not known.

$$J(\alpha; \frac{\pi}{2}) = J_0 = Const. \quad (B1)$$

Thus, Eq. (22) reduces to

$$\frac{d\theta_c}{dt}\left(\frac{\pi}{2}\right) = -\frac{J_0}{R\rho_{drop}} \frac{\pi}{2}. \quad (\text{B2})$$

Consequently,

$$f(\alpha; \frac{\pi}{2}) = \frac{RJ_0}{\rho_{drop}} \left[\frac{\pi}{2} (\tanh \alpha - 1) + \sin^{-1} \left(\frac{1}{\cosh \alpha} \right) \right] \quad (\text{B3})$$

and

$$h(\alpha; \frac{\pi}{2}) = -\frac{RJ_0}{\rho_{drop}} \tanh \alpha. \quad (\text{B4})$$

Using Fourier sine transform,

$$k(\tau; \frac{\pi}{2}) = \frac{RJ_0}{\rho_{drop}} \times \left[-\frac{\tau}{1+\tau^2} + \frac{2}{\pi} \int_0^\infty \cosh \alpha \sin^{-1} \left(\frac{1}{\cosh \alpha} \right) \sin(\tau \alpha) d\alpha \right] \quad (\text{B5})$$

and

$$\kappa(\tau; \frac{\pi}{2}) = -\frac{RJ_0}{\rho_{drop}} \times \frac{1}{\sinh(\frac{\pi}{2} \tau)}. \quad (\text{B6})$$

For hemisphere case from [13] it is known that

$$J(\alpha, \theta_c) = \frac{\rho_{mix} D_{AB} (u_\infty - u_s)}{R}. \quad (\text{B7})$$

Thus, Eq. (19) becomes

$$\frac{d\theta_c}{dt}\left(\frac{\pi}{2}\right) = \frac{\rho_{mix} D_{AB} (u_s - u_\infty)}{\rho_{drop} R^2} \times 2. \quad (\text{B8})$$

Consequently,

$$f(\alpha; \frac{\pi}{2}) = \frac{\rho_{mix} D_{AB} R (u_\infty - u_s)}{\rho_{drop}} \times \left(\frac{1}{\cosh \alpha} - \frac{1}{\cosh^2 \alpha} \right) \quad (\text{B9})$$

and

$$h(\alpha; \frac{\pi}{2}) = \frac{\rho_{mix} D_{AB} R(u_{\infty} - u_s)}{\rho_{drop}} \left(\frac{1.75}{\cosh^{1.5} \alpha} - \frac{0.75}{\cosh^{2.5} \alpha} - \sqrt{\cosh \alpha} \right). \quad (B10)$$

Using transform table provided in the previous work [8],

$$k(\tau; \frac{\pi}{2}) = -\frac{\rho_{mix} D_{AB} R(u_{\infty} - u_s)}{\rho_{drop}} \times \tau \tanh(\pi\tau) \left[\frac{1}{2\sqrt{2}\tau \sinh(\frac{\pi}{2}\tau)} + \frac{1}{\sqrt{2} \cosh(\frac{\pi}{2}\tau)} \right] \quad (B11)$$

and

$$\kappa(\tau; \frac{\pi}{2}) = \frac{\rho_{mix} D_{AB} R(u_{\infty} - u_s)}{\rho_{drop}} \times \left[\frac{1}{\sinh(\frac{\pi}{2}\tau)} \left(1.75\sqrt{2}\tau + \frac{1}{2\sqrt{2}\tau} \right) - \frac{\sqrt{2}(\tau^2 + 1)}{2 \cosh(\frac{\pi}{2}\tau)} \right]. \quad (B12)$$

REFERENCES

- [1] N. R. Bieri, J. Chung, S. E. Haferl, et al., Applied Physics Letters **82**, 3529 (2003).
- [2] H. Cong and W. X. Cao, Langmuir **19**, 8177 (2003).
- [3] F. Q. Fan and K. J. Stebe, Langmuir **20**, 3062 (2004).
- [4] E. Widjaja and M. T. Harris, Computers & Chemical Engineering **In Press**, **Corrected Proof** (2008).
- [5] Y. Y. Tarasevich, Physical Review E **71** (2005).
- [6] A. J. Petsi and V. N. Burganos, Physical Review E **72** (2005).
- [7] A. J. Petsi and V. N. Burganos, Physical Review E **73** (2006).
- [8] H. Masoud, Physical Review E, **In review** (2008).
- [9] B. J. Fischer, Langmuir **18**, 60 (2002).
- [10] H. Hu and R. G. Larson, Langmuir **21**, 3963 (2005).

- [11] E. Widjaja and M. T. Harris, Computers & Chemical Engineering **In Press**, **Corrected Proof** (2008).
- [12] R. D. Deegan, O. Bakajin, T. F. Dupont, et al., Physical Review E **62**, 756 (2000).
- [13] Y. O. Popov, Physical Review E **71** (2005).
- [14] N. A. Fuchs, *Evaporation and droplet growth in gaseous media* (Pergamon Press, London, New York,, 1959).
- [15] D. M. Anderson and S. H. Davis, Physics of Fluids **7**, 248 (1995).
- [16] H. Hu and R. G. Larson, Journal of Physical Chemistry B **106**, 1334 (2002).
- [17] A. L. Yarin, J. B. Szczech, C. M. Megaridis, et al., Journal of Colloid and Interface Science **294**, 343 (2006).
- [18] J. Happel and H. Brenner, *Low Reynolds number hydrodynamics : with special applications to particulate media* (M. Nijhoff ; Distributed by Kluwer Boston, The Hague ; Boston Hingham, MA, USA, 1983).
- [19] N. N. Lebedev and R. A. Silverman, *Special functions and their applications* (Prentice-Hall, Englewood Cliffs, N.J., 1965).
- [20] I. N. Sneddon, *The use of integral transforms* (McGraw-Hill, New York, 1972).
- [21] G. B. Jeffery, Philosophical Transactions of the Royal Society of London. Series A, Containing Papers of a Mathematical or Physical Character **221**, 265 (1921).
- [22] M. Stimson and G. B. Jeffery, Proceedings of the Royal Society of London. Series A, Containing Papers of a Mathematical and Physical Character **111**, 110 (1926).
- [23] G. Guena, C. Poulard, and A. M. Cazabat, Journal of Colloid and Interface Science **312**, 164 (2007).